Wireless Networks (2018) 24:2781–2794
https://doi.org/10.1007/s11276-017-1634-7

# A novel spectrum sensing scheme with sensing time optimization for energy-efficient CRSNs

Fanhua Kong[1] · Zilong Jin[2] · Jinsung Cho[1] · Ben Lee[3]

Published online: 1 December 2017


**Abstract**
The cognitive radio technology enables secondary users (SUs) to occupy licensed bands when primary users (PUs) are not occupy them. Spectrum sensing is a key technology for SUs to detect PUs, and the sensing time is a critical parameter for spectrum sensing performance. Optimum sensing time tradeoffs between the spectrum sensing performance and the secondary throughput. This paper proposes a novel spectrum sensing scheme that performs spectrum sensing for either one period or two periods based on the previous sensing result. Due to the energy constraint in cognitive radio sensor networks, the energy efficiency is maximized by optimizing spectrum sensing time. In order to seek the optimal sensing time, the objective function is proven to be a concave function and the Golden Section Search method is employed. Our simulation study verifies that the proposed scheme improves the network energy efficiency, especially when PUs are more active.

**Keywords** Cognitive radio sensor networks · Sensing time · Energy efficiency · Golden section search method

## 1 Introduction

Due to the fixed spectrum allocation policy and the rapid deployment of wireless devices, the problem of spectrum scarcity is becoming more severe. Nevertheless, Federal Communications Commission (FCC) has reported that most licensed wireless spectrum bands are underutilized [1]. Recently, cognitive radio (CR) technologies have been proposed to alleviate the spectrum scarcity problem [2]. CR has attracted a lot of attention because it allows unlicensed secondary users (SUs) to opportunistically access the licensed bands when licensed primary users (PUs) are not occupying them. Due to this benefit, CR technologies have been extensively applied in various wireless networks to improve spectral efficiency [3–5].

SUs utilizing CR technologies can find *spectrum holes* or *white spaces*, and share the licensed bands with PUs in a collision-free manner. Figure 1 presents a simple cognitive radio network (CRN), where the PU has higher priority for occupying the licensed bands. The shaded area indicates the communication range of the PU, and the solid and the dashed arrows represent the data transmission between SUs and the PU detection, respectively. When the SUs in the shaded area detect that the PU is busy, they cannot occupy the licensed band and communicate with other SUs. If the SUs detect that the PU is not busy, they can transmit data (using RTS/CTS or other methods to coordinate the communications among SUs). Figure 1 shows a simple CRN with one PU and several SUs. However, if there are more than one PU, SUs must perform spectrum sensing on all the licensed bands they occupy. Thus, it is very important for SUs to accurately determine whether or not PUs are present. *Spectrum sensing* is the key technology used to detect PUs, and the amount of time spent sensing is a critical parameter for performance. The optimal sensing time

✉ Jinsung Cho
chojs@khu.ac.kr

Fanhua Kong
kongfanhua@khu.ac.kr

Zilong Jin
zljin@nuist.edu.cn

Ben Lee
benl@eecs.oregonstate.edu

[1] Department of Computer Science and Engineering, Kyung Hee University, Yongin 446-701, Republic of Korea

[2] School of Computer and Software, Nanjing University of Information Science and Technology, Nanjing 210044, China

[3] School of Electrical Engineering and Computer Science, Oregon State University, Corvallis, OR 97331, USA

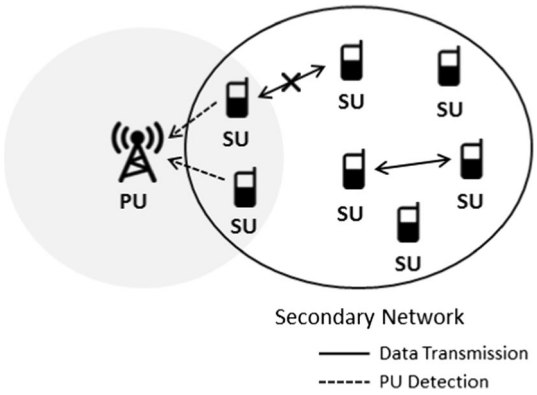


**Fig. 1** Architecture of cognitive radio network

trades off between the detection accuracy and the achieved secondary throughput. More specifically, a longer spectrum sensing time leads to better sensing accuracy, but less time remains for data transmission degrading the throughput of the secondary network.

For the optimum spectrum sensing time, miss detection and false alarm probabilities are the main performance metrics. A *miss detection* occurs when an SU fails to detect a PU that is present. A *false alarm* occurs when an SU detects a PU when it is actually absent. If a miss detection occurs, the communications by SUs will interfere with the PUs' communications. As a result, PUs can have better protection from interference if miss detection probability is lower. From the perspective of SUs, if the probability of false alarm is lower, opportunities for SUs to utilize spectrum holes for data transmission become higher and the secondary throughput will increase. A longer sensing time will lead to a lower miss detection probability (i.e., higher detection probability) but a higher false alarm probability (see Sect. 4.1).

Energy consumption is the most important factor in CRSNs, where low-cost, battery-powered sensor nodes are dispersed in a specific area to satisfy various applications, including environment monitoring, surveillance, health care, and battlefield control [6]. Due to the application environment, it is hard or impossible to change or recharge the batteries for the sensor nodes. Therefore, improving energy efficiency and prolonging the network lifetime is the most crucial issue for the development of CRSNs.

Therefore, this paper proposes a novel spectrum sensing scheme to improve the energy efficiency of CRSNs. The proposed scheme takes into consideration the previous sensing result. If the sensing result of the current frame is the same as the sensing result of the previous frame, the SU simply performs a spectrum sensing once. Otherwise, the SU will perform spectrum sensing for a second time to ensure the correctness of the first sensing result. There are two main advantages to the proposed method:

(a) If a PU is actually absent during both the previous and the current frames and a *false alarm* occurs during the first spectrum sensing of the current frame, then the probability that the sensing error can be corrected during the second spectrum sensing increases. As a result, the secondary throughput can be improved.
(b) If a PU is actually present during both the previous and the current frames and a *miss detection* occurs during the first spectrum sensing of the current frame, then the probability that the sensing error can be corrected during the second spectrum sensing increases. As a result, PU can have a better protection from interference and energy efficiency can be improved by reducing the number of invalid transmissions due to miss detection.

Our simulation study validates that the proposed scheme reduces sensing errors and improves network energy efficiency, especially when PUs are relatively active.

The rest of the paper is organized as follows. Section 2 discusses the related work. Section 3 presents the system model of the proposed method. In Sect. 4, an optimization problem is formulated to obtain the optimal sensing time. In Sect. 5, the performance of the proposed scheme is evaluated using simulations. Finally, Sect. 6 concludes the paper and discusses a possible future work.

## 2 Related work

Some recent work on sensing time optimization for CRNs have been presented in [7–12]. Ewaisha et al. [7] investigated a joint optimization of sensing time, decision threshold, and channel sensing order. They derived a reward function that includes a negative term to penalize collisions with PUs, and the secondary throughput is maximized by finding the optimal solution for the reward function. In this work, the channels are sensed in order and for each channel sensed to be idle, its capacity will be compared with the capacity of the next idle channel. Then, the channel with the highest capacity is selected for data transmission. However, the state of channel occupancy is not considered when the channel sensing order is determined. If the channel with the highest capacity is frequently occupied by the PU, more time and energy will be wasted to search for the optimal channel for data transmission. Hao et al. [8] developed an adaptive spectrum sensing scheme to maximize the average throughput. Their work considered time-varying channels, and adjusted the missing transmission probability to improve the average throughput. More specifically, the missing transmission

probability is reduced when the channel is good and the missing transmission probability is increased when the channel is bad. The current channel state is predicted based on the previous sensing results and the channel state information, and the sensing time is adjusted accordingly. This work assumes that the channel state information can only be obtained after the spectrum sensing is completed and the sensing result indicates the channel is idle. This way, if the PU rarely occupies the channel, more time and energy will be needed to predict the current channel state before each spectrum sensing and data transmission. Shokri-Ghadikolaei et al. [9] proposed a learning-based sensing time optimization scheme to maximize the average throughput. More specifically, a multilayer feedforward neural network is utilized for learning the actual behavior of the secondary link, and based on this, a Kennedy-Chua neural network is employed to find the optimal sensing time. This work assumes that an SU senses several channels in order until a transmission opportunity is found. However, the authors only focus on sensing time optimization and optimizing the channel sensing order is ignored. An inappropriate channel sensing order will require more time and energy to search the channel for data transmission. Sun et al. [10] investigated the tradeoff between sensing accuracy and secondary throughput for cooperative spectrum sensing based on soft decision. They analyzed the impact different system parameters have on the optimal sensing time, and showed that these can lead to different results. Liu et al. [11] investigated a joint optimization of the sensing time and the number of cooperative users, which maximized CRN throughput subject to the constraints of both false alarm and miss detection probabilities. Yin et al. [12] proposed a joint sensing-time adaption and data transmission scheme to improve spectrum utilization and throughput. Their method bundles two adjacent sensing periods to form a sensing block. At first, an SU performs a partial spectrum sensing, and if a PU is not detected, it transmits data; otherwise, a full spectrum sensing is performed. However, all the aforementioned techniques are specific to CRNs and they do not consider energy restriction for CRSNs. Therefore, these technologies cannot be directly applied to CRSNs.

Zhong et al. [13] investigated a joint optimal energy-efficient cooperative spectrum sensing and transmission in a multi-channel CR system. The network energy efficiency is maximized by jointly optimizing the sensing time, the number of cooperative sensing SUs, and the transmission bandwidth. However, the authors optimize the number of cooperative sensing SUs using the exhaustive search method, and then investigate the optimum sensing time, transmission bandwidth and power. If the network consists of hundreds of SUs, the computational complexity will be high. Luo et al. [14] proposed a scheme that minimizes the mean sensing time with the goal of meeting the basic requirements of a secondary network, i.e., the detection probability must not be smaller than a pre-defined threshold and the false alarm probability must not be larger than a pre-defined threshold. Their scheme minimizes the spectrum sensing time, and thus maximizes the time remaining for data transmission. They show that the minimum average sensing time can be attained when the false alarm probability reaches its threshold. However, even though the maximum time is left for data transmission, the probability of sensing errors becomes high due to the low detection probability and the high false alarm probability. This will cause more interference to the PU and lose more opportunities for data transmission.

In terms of CRSNs, Deepak et al. [15] proposed a method based on cognitive monitoring network, where a separate network of sensors is deployed to perform cooperative spectrum sensing within a network coverage area. Thus, instead of performing spectrum sensing, SUs spend a short amount of time to send query to and then receive sensing results from monitoring sensors. This allows the secondary throughput to be maximized irrespective of the sensing duration. However, the delay due the communication between SUs and monitoring sensors will increase. In addition, monitoring sensors will expend energy for spectrum sensing. Jiang et al. [16] investigated an energy-efficient optimization method for spectrum sensing and node selection. In this work, a dynamic censored spectrum sensing scheme is employed, where each sensor node compares the received power with a censoring threshold, and then decides when to stop sensing. This way, the sensing time can be reduced and unnecessary sensing energy consumption can be avoided. However, if a sensor node collects just a few samples and then stops spectrum sensing, the probability of sensing error will increase.

Awin et al. [17] investigated a joint optimal transmission power and sensing time for energy-efficient spectrum sensing. The optimization problem is formulated as a function of two variables (i.e., transmission power and sensing time) subjected to PU protection constraints. An iterative algorithm is applied to determine the optimal transmission power and sensing time that maximizes the energy efficiency of a CR system. Zhang et al. [18] also investigated the power control and sensing time optimization problem for energy efficient cognitive small cell network. The cross-tier interference mitigation, imperfect hybrid spectrum sensing, and energy efficiency are considered. A hybrid spectrum sensing that combines spectrum sharing access and opportunistic spectrum access is considered in the optimization problem. An iterative resource allocation algorithm is developed to achieve the optimal sensing time and power allocation, which in turn maximizes the energy efficiency. Li et al. [19] proposed an

energy-efficient technique for cooperative spectrum sensing. In their method, all SUs perform cooperative spectrum sensing for one period. If the sensing result shows that the PU is absent, SUs will transmit data. The optimal sensing time is attained by optimizing the ratio of the secondary throughput and the total energy consumption. However, the work in [17–19] perform spectrum sensing just once and then find the optimal sensing time that maximizes the network energy efficiency. If miss detections and false alarms occur, there is no opportunity to correct these sensing errors. This will cause interference and the available spectrum opportunities will be wasted. In our proposed scheme, spectrum sensing will be performed again when the sensing results of the current and previous frames are different. This allows the sensing errors have a certain probability to be corrected.

## 3 System model

This paper considers a CRSN consisting of a single PU and multiple SUs communicating on a licensed band, which is subdivided into several non-overlapping sub-bands. Moreover, an SU is assigned to a sub-band to sense whether it is occupied by the PU. Time is divided into equal sized frames, where each frame consists of two phases: the *sensing* phase and the *data transmission* phase. Each SU performs spectrum sensing during the sensing phase to detect the PU. Each SU will transmit data if the PU is detected to be idle or absent; otherwise, it will keep silent and wait for the next frame. Furthermore, each SU is assumed to always have data to transmit if the sensing result shows that the PU is absent. If the sensing results of the current and previous frames are the same, an SU simply performs spectrum sensing only once for the current frame. If the sensing result of the current frame is different from the sensing result of the previous frame, an SU will perform another spectrum sensing to ensure the accuracy of the first sensing result. Note that if the first and the second sensing results of the current frame are different, the second sensing result will be taken as the final sensing decision, even if it is wrong. This can occur because the spectrum sensing is not perfect, and thus an SU may not be able to ascertain the actual states of the PU. The spectrum sensing accuracy is related to the miss detection and false alarm probabilities. Therefore, in order to simplify the proposed scheme, the sensing result of the previous frame is considered as the correct state (i.e., the actual state of the PU), even though it may be wrong.

Figure 2 shows the frame structure of the proposed scheme. The fame length is $T$ and $t_1$ and $t_2$ represent the first and the second spectrum sensing period, respectively. As mentioned before, if the first and the second sensing

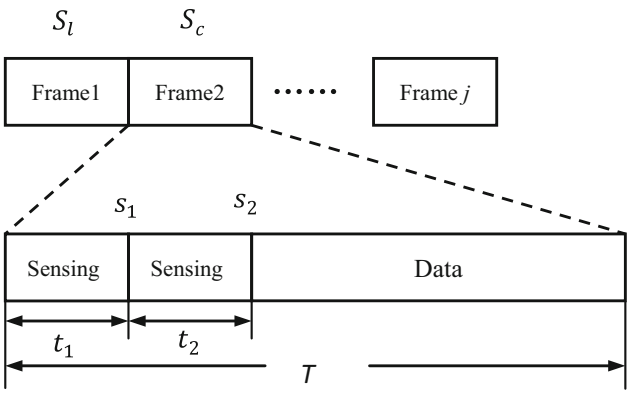


**Fig. 2** Frame structure

results of the current frame are different, the second sensing result will be taken as the final sensing decision. Since the longer sensing time can lead to a better sensing performance, the condition $t_2 \geq t_1$ is imposed to increase the accuracy of the second sensing result. In addition, $S_l$ and $S_c$ represent the actual state of PU for the previous and the current frame, respectively, and $s_1$ and $s_2$ denote the first and the second sensing results of the current frame, respectively. The variables $S_l$, $S_c$, $s_1$, and $s_2$ are assigned 0 and 1 to represent the absence and presence of a PU, respectively, and thus have the following meanings:

$S_l = 0$ or 1: PU was idle or busy in the previous frame.
$S_c = 0$ or 1: PU is idle or busy in the current frame.
$s_1 = 0$ or 1: The first sensing result of the current frame indicating that PU is idle or busy.
$s_2 = 0$ or 1: The second sensing result of the current frame indicating that PU is idle or busy.

Based on $S_l$, $S_c$, $s_1$, and $s_2$, there are 12 possible cases considered by the proposed scheme:

*Case 1* ($S_l = 0$, $S_c = 0$, $s_1 = 0$) The PU is idle during both the previous and the current frames, and the SU detects that the PU is idle during $t_1$. Since the sensing result ($s_1 = 0$) is the same as the previous frame ($S_l = 0$), the SU will perform spectrum sensing only once, and then transmit data during the time period $T - t_1$.

*Case 2* ($S_l = 0$, $S_c = 0$, $s_1 = 1$, $s_2 = 0$) The PU is idle during both the previous and the current frames, but a false alarm occurs and the SU detects that the PU is busy during $t_1$. Since the first sensing result ($s_1 = 1$) is different from the previous frame ($S_l = 0$), the SU will perform spectrum sensing again during $t_2$. The second sensing result ($s_2 = 0$) is taken as the final sensing result. Since the final sensing result shows that the PU is idle, the SU will transmit data during the time period $T - t_1 - t_2$. Even though a false alarm occurred during $t_1$, this error can be corrected during $t_2$ and, as a consequence, higher secondary throughput will be achieved.

*Case 3* ($S_l = 0$, $S_c = 0$, $s_1 = 1$, $s_2 = 1$) A false alarm occurs during both $t_1$ and $t_2$. The SU will keep silent and wait for the next frame, and thus there is no secondary throughput.

*Case 4* ($S_l = 1$, $S_c = 0$, $s_1 = 0$, $s_2 = 1$) The first sensing result ($s_1 = 0$) is different from the final sensing result of the previous frame ($S_l = 1$), thus the SU will perform spectrum sensing again during $t_2$. However, a false alarm occurs during $t_2$. Therefore, the SU will keep silent and wait for the next frame, and thus there is no secondary throughput.

*Case 5* ($S_l = 1$, $S_c = 0$, $s_1 = 0$, $s_2 = 0$) The SU performs spectrum sensing during $t_1$ and $t_2$, and both sensing results indicate that the PU is absent. The data will be successfully transmitted.

*Case 6* ($S_l = 1$, $S_c = 0$, $s_1 = 1$) A false alarm occurs during $t_1$. Nonetheless, the first sensing result ($s_1 = 1$) is the same as the previous frame ($S_l = 1$), thus the SU will not perform spectrum sensing again. The SU will keep silent and wait for the next frame, and thus there is no secondary throughput.

*Case 7* ($S_l = 1$, $S_c = 1$, $s_1 = 0$, $s_2 = 1$) A miss detection occurs during $t_1$ and the first sensing result ($s_1 = 0$) is different from the previous frame ($S_l = 1$), but the PU is detected during $t_2$. As a consequence, a better protection is provided against miss detection and more energy will be saved.

*Case 8* ($S_l = 1$, $S_c = 1$, $s_1 = 0$, $s_2 = 0$) A miss detection occurs during $t_1$ and $t_2$. Since the SU failed to detect the PU, it will transmit data. However, the data transmission will fail and there will be no secondary throughput.

*Case 9* ($S_l = 1$, $S_c = 1$, $s_1 = 1$) The SU successfully detects the PU, and it will remain silent and wait for the next frame.

*Case 10* ($S_l = 0$, $S_c = 1$, $s_1 = 0$) A miss detection occurs during $t_1$ and the sensing result ($s_1 = 0$) is the same as the previous frame ($S_l = 0$), thus spectrum sensing will be performed only once. Since data transmission is successful only when the PU is actually absent, there will be no secondary throughput.

*Case 11* ($S_l = 0$, $S_c = 1$, $s_1 = 1$, $s_2 = 0$) The SU detects the PU during $t_1$. Since the sensing result ($s_1 = 1$) is different from the sensing result of the previous frame ($S_l = 0$), the SU performs spectrum sensing again, and a miss detection occurs during $t_2$. Therefore, the data transmission will fail and there will be no secondary throughput.

*Case 12* ($S_l = 0$, $S_c = 1$, $s_1 = 1$, $s_2 = 1$) The SU successfully detects the PU during $t_1$ and $t_2$, and thus it will remain silent and wait for the next frame.

Based on the aforementioned cases, the valid secondary throughput can be achieved only for cases 1, 2 and 5, while cases 3, 4 and 6 will lead to false alarm. Cases 7, 9 and 12 can successfully detect the PU, while cases 8, 10, and 11 will cause miss detection. The summary of 12 cases is presented in Table 1, which also includes for each case whether or not false alarm (FA), miss detection (MD), and valid throughput (TP) occur.

## 4 Problem formulation

This section analyzes how sensing time affects the sensing accuracy and the secondary throughput by developing an analytical model. The main objective of the analysis is to find an optimal sensing time that maximizes network energy efficiency as well as yields good sensing accuracy.

### 4.1 Energy detector based spectrum sensing

Our analysis uses a binary hypothesis to formulate the spectrum sensing. Let $H_0$ and $H_1$ denote the hypothesis of the idle and busy states of a PU, respectively. The probabilities of $H_0$ and $H_1$ are denoted as $p_0$ and $p_1$, respectively, and $p_0 + p_1 = 1$. In the proposed scheme, the PU's spectrum occupancy is assumed to follow a Markov chain model shown in Fig. 3. The existence of a Markov chain for the spectrum occupancy by PUs has been validated in [20]. The state space of the Markov process is $X = \{H_0, H_1\}$, where $H_0 = 0$ and $H_1 = 1$. As shown in Fig. 3, $q_n$ which denotes the actual state of PU can be 0 or 1 (i.e., $H_0$ or $H_1$). The state transition probability matrix A is defined as $\mathrm{A} = \{a_{ij}\}$, $a_{ij} = P(q_{n+1} = j | q_n = i)$ for $i, j \in X$, where $q_n$ and $q_{n+1}$ denote the actual states of PU in $n$th and $(n+1)$st frame, respectively. More specifically, $a_{00}$ and $a_{11}$ denote the probabilities that the state of PU maintains $H_0$ and $H_1$ from the current frame to the next frame, respectively. $a_{01}$ and $a_{10}$ denote the probabilities

**Table 1** Summary of spectrum sensing cases

| Cases | State | | | | Outcome | | |
|---|---|---|---|---|---|---|---|
| | $S_l$ | $S_c$ | $s_1$ | $s_2$ | FA | MD | TP |
| 1 | 0 | 0 | 0 | N/A | N | N | Y |
| 2 | 0 | 0 | 1 | 0 | N | N | Y |
| 3 | 0 | 0 | 1 | 1 | Y | N | N |
| 4 | 1 | 0 | 0 | 1 | Y | N | N |
| 5 | 1 | 0 | 0 | 0 | N | N | Y |
| 6 | 1 | 0 | 1 | N/A | Y | N | N |
| 7 | 1 | 1 | 0 | 1 | N | N | N |
| 8 | 1 | 1 | 0 | 0 | N | Y | N |
| 9 | 1 | 1 | 1 | N/A | N | N | N |
| 10 | 0 | 1 | 0 | N/A | N | Y | N |
| 11 | 0 | 1 | 1 | 0 | N | Y | N |
| 12 | 0 | 1 | 1 | 1 | N | N | N |

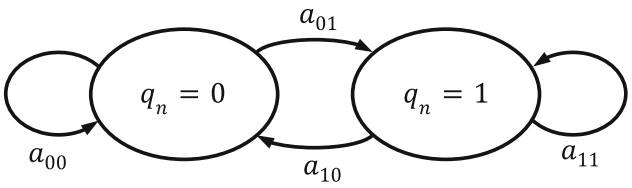


**Fig. 3** Markov model for spectrum occupancy of PUs

that the state of PU becomes $H_1$ from $H_0$ and $H_0$ from $H_1$ in the next frame, respectively. In addition, $a_{00} = a_{10} = p_0$ and $a_{01} = a_{11} = p_1$ are assumed. Moreover, the busy and idle periods of PU are assumed to be longer than the frame length. As a consequence, the probability that the state of PU changes more than once in a frame is negligible.

In order to maximize the secondary throughput and at the same time provide some desired level of protection to PU, $t_1$ needs to be minimized. Moreover, if a false alarm or a miss detection occurs, the second spectrum sensing time $t_2$ provides an opportunity to correct the sensing errors with a certain probability to improve performance. Therefore, $t_1$ can be expressed in terms of detection probability, $p_d$, and false alarm probability, $p_f$, as follows:

$$\min t_1 \; s.t. \; p_d \geq p_d^{th}, p_f \leq p_f^{th}, \tag{1}$$

where $p_d^{th}$ and $p_f^{th}$ represent the respective predefined thresholds that guarantee the necessary protection against interference and secondary throughput for PUs.

Due to the energy constraint in CRSNs, the value of $t_2$ can be calculated by maximizing the network energy efficiency. The proposed method utilizes an energy detector for spectrum sensing, which is widely used due to its simplicity and requires no prior knowledge of PUs [21–23]. The test statistic of an energy detector $T(y)$ can be calculated as follows:

$$T(y) = \frac{1}{\sigma_u^2} \sum_{n=1}^{N} |y(n)|^2, \tag{2}$$

where $N$ is the number of samples performed during the sensing phase and $y(n)$ is the sampled signal. When the state of PU is $H_0$, then $y(n) = u(n)$, where $u(n)$ is the noise, which is a Gaussian iid random process with mean of zero and variance of $\sigma_u^2$. On the other hand, when the state of PU is $H_1$, $y(n) = s(n) + u(n)$, where $s(n)$ is the signal of PU, which is an iid random process with mean of zero and variance of $\sigma_s^2$. The test statistic follows the central and non-central Chi square distribution with $2N$ degrees of freedom under the hypotheses $H_0$ and $H_1$, respectively [24]. The test statistic can be approximated as a Gaussian random process because the central limit theorem can be utilized when the value of $N$ is sufficiently large [25], and thus $T(y)$ is given by

$$T(y) \sim \begin{matrix} \mathcal{N}(N, 2N) & H_0 \\ \mathcal{N}\left(N(1+\gamma), 2N(1+\gamma)^2\right) & H_1 \end{matrix}, \tag{3}$$

where $\gamma = \frac{\sigma_s^2}{\sigma_u^2}$ is the received signal to noise ratio (SNR) from PU for PU detection. The detection probability $p_d$ and the false alarm probability $p_f$ can be expressed by

$$p_d = p(H_1|H_1), \tag{4}$$

$$p_f = p(H_1|H_0). \tag{5}$$

The miss detection is defined as when SU does not detect the presence of PU when PU is actually present. Therefore, the miss detection probability $p_m$ can be expressed as $p_1(1 - p_d)$. Based on the test statistics of $T(y)$, the detection probability $p_d = p(T(y) > \lambda|H_1)$ and the false alarm probability $p_f = p(T(y) > \lambda|H_0)$ can be evaluated in terms of Q-function as [12, 26]:

$$p_d = \mathcal{Q}\left(\frac{\lambda}{\sqrt{2N}(1+\gamma)} - \sqrt{\frac{N}{2}}\right), \tag{6}$$

$$p_f = \mathcal{Q}\left(\frac{\lambda}{\sqrt{2N}} - \sqrt{\frac{N}{2}}\right), \tag{7}$$

where $\lambda$ is the sensing threshold. If the received power is higher than $\lambda$, PU is considered to be busy; otherwise, PU is considered to be idle. $\mathcal{Q}(\cdot)$ is the Q-function given as

$$\mathcal{Q}(x) = \frac{1}{\sqrt{2\pi}} \int_x^{\infty} \exp\left(-\frac{u^2}{2}\right) du. \tag{8}$$

The number of samples $N$ can be represented by the following equation [24]:

$$N = 2tW, \tag{9}$$

where $t$ is the sensing time and $W$ is the bandwidth of the PU signal. Since $\mathcal{Q}(x)$ is a monotonically decreasing function, both $p_d$ and $p_f$ will increase as sensing time increases. The sensing threshold $\lambda$ can be calculated using Eq. (6) as shown below:

$$\lambda = \sqrt{2N}(1+\gamma)\left(\mathcal{Q}^{-1}(p_d) + \sqrt{\frac{N}{2}}\right). \tag{10}$$

Substituting Eqs. (9) and (10) into Eq. (7) leads to the following equation for $p_f$:

$$p_f = \mathcal{Q}\left((1+\gamma)\mathcal{Q}^{-1}(p_d) + \gamma\sqrt{tW}\right). \tag{11}$$

According to Eq. (11), $p_f$ decreases as $p_d$ decreases. Since the objective is to maximize the secondary throughput and at the same time provide protection for PU from interference, the detection probability during $t_1$, $p_d^1$, is

set equal to $p_d^{th}$. As mentioned earlier, $t_1$ can be calculated based on Eq. (1) subject to the constraint $p_f \le p_f^{th}$. Thus, when $p_f$ for $t_1$ equals to $p_f^{th}$, $t_1$ is minimized. Therefore, solving Eq. (11) for $t$ with $p_f$ set to $p_f^{th}$ and $p_d$ set to $p_d^{th}$ leads to the following equation for $t_1$:

$$t_1 = \frac{\left(\left(Q^{-1}\left(p_f^{th}\right) - (1+\gamma)Q^{-1}\left(p_d^{th}\right)\right)/\gamma\right)^2}{W}. \quad (12)$$

As mentioned earlier, $t_2$ can be calculated by maximizing the network energy efficiency. In the following subsection, an analytical model is developed to seek the optimal value of $t_2$. In the proposed scheme, the detection probability for $t_2$, $p_d^2$, is also fixed at $p_d^{th}$. As previously mentioned, $t_2$ should not be smaller than $t_1$. Since $Q$ in Eq. (11) is a decreasing function, $p_f$ decreases as sensing time $t$ increases, i.e., $p_f^2 \le p_f^1$, where $p_f^1$ and $p_f^2$ denote the false alarm probabilities of $t_1$ and $t_2$, respectively. Thus, the sensing accuracy of $t_2$ is better. This is the reason why the sensing result of $t_2$ is taken as the final sensing result if it is different from the sensing result of $t_1$.

### 4.2 Problem formulation

Among the 12 possible cases discussed in Sect. 3, the ones that provide valid secondary throughput are cases 1, 2 and 5, which are denoted as $R_1$, $R_2$, and $R_5$, respectively, and are represented as follows:

$$R_1 = p_0^2\left(1-p_f^1\right)(T-t_1)C, \quad (13a)$$

$$R_2 = p_0^2 p_f^1\left(1-p_f^2\right)(T-t_1-t_2)C, \quad (13b)$$

$$R_5 = p_1 p_0\left(1-p_f^1\right)\left(1-p_f^2\right)(T-t_1-t_2)C, \quad (13c)$$

where $C$ denotes the channel capacity under the hypothesis $H_0$. According to Shannon theory, $C$ can be calculated by

$$C = \log_2(1+\gamma_s). \quad (14)$$

where $\gamma_s$ is the SNR received from the SU transmitter.

The total average secondary throughput $R_{total}$ is then given by

$$R_{total} = R_1 + R_2 + R_5. \quad (15)$$

Based on the above discussion, the energy consumption for the 12 cases, $E_{1-12}$, and the total average energy consumption, $E_{total}$, can be expressed as follows:

$$E_1 = p_0^2\left(1-p_f^1\right)(t_1E_s + (T-t_1)E_t), \quad (16a)$$

$$E_2 = p_0^2 p_f^1\left(1-p_f^2\right)((t_1+t_2)E_s + (T-t_1-t_2)E_t), \quad (16b)$$

$$E_3 = p_0^2 p_f^1 p_f^2 (t_1+t_2)E_s, \quad (16c)$$

$$E_4 = p_1 p_0 p_f^2\left(1-p_f^1\right)(t_1+t_2)E_s, \quad (16d)$$

$$E_5 = p_1 p_0\left(1-p_f^1\right)\left(1-p_f^2\right)((t_1+t_2)E_s + (T-t_1-t_2)E_t), \quad (16e)$$

$$E_6 = p_1 p_0 p_f^1 t_1 E_s, \quad (16f)$$

$$E_7 = p_1^2 p_d^1\left(1-p_d^2\right)(t_1+t_2)E_s, \quad (16g)$$

$$E_8 = p_1^2\left(1-p_d^1\right)\left(1-p_d^2\right)((t_1+t_2)E_s + (T-t_1-t_2)E_t), \quad (16h)$$

$$E_9 = p_1^2 p_d^1 t_1 E_s, \quad (16i)$$

$$E_{10} = p_0 p_1\left(1-p_d^1\right)(t_1E_s + (T-t_1)E_t), \quad (16j)$$

$$E_{11} = p_0 p_1 p_d^1\left(1-p_d^2\right)((t_1+t_2)E_s + (T-t_1-t_2)E_t), \quad (16k)$$

$$E_{12} = p_0 p_1 p_d^1 p_d^2 (t_1+t_2)E_s, \quad (16l)$$

$$E_{total} = E_1 + E_2 + E_3 + E_4 + E_5 + E_6 + E_7 + E_8 + E_9 + E_{10} + E_{11} + E_{12}, \quad (16m)$$

where $E_s$ and $E_t$ are the energy consumed by spectrum sensing and data transmission for unit time, respectively.

In this paper, energy efficiency is defined as the number of bits transmitted per unit of energy consumption [27]. Therefore, the objective function of energy efficiency $\eta$ can be expressed as:

$$\eta = \frac{R_{total}}{E_{total}}. \quad (17)$$

In Eq. (17), $t_2$ is the only unknown variable. The value of $t_2$ that maximizes the function $\eta$ is the optimal sensing time. As mentioned before, the second sensing result will be taken as the final sensing decision when the first and the second sensing results of the current frame are different. Therefore, the condition $t_2 \ge t_1$ is assumed to increase the accuracy of the second sensing result. Moreover, since the frame time is set as $T$, $t_2$ must satisfy the constraint $t_1 \le t_2 \le T$. In addition, since both $p_d^1$ and $p_d^2$ are fixed at $p_d^{\text{th}}$, $p_f^2$ must also satisfy the constraint $p_f^2 \le p_f^{th}$ to guarantee the requirement of secondary throughput for CRSNs when the optimal value of $t_2$ is calculated. Therefore, the maximization problem can be formulated as follows:

$$\max \eta(t_2)\ s.t.\ t_1 \le t_2 \le T, p_f^2 \le p_f^{th}. \quad (18)$$

### 4.3 Golden section search method

In order to determine the optimal value of $t_2$, the Golden Section Search method is applied to find the extremum (minimum or maximum) of a unimodal function. This subsection proves that the objective function $\eta(t_2)$ is a concave function, and the Golden Section Search method can be used to find the optimal value of $t_2$ that maximizes the energy efficiency.

Based on Eq. (15), the second derivative of $R_{total}$ can be calculated as follows:

$$R_{total}^{''} = R_1^{''} + R_2^{''} + R_5^{''}, \tag{19}$$

where $R_1^{''}$, $R_2^{''}$, and $R_5^{''}$ are the second derivatives of $R_1$, $R_2$, and $R_5$ in terms of $t_2$, respectively. According to Eqs. (13a), (13b), and (13c), $R_1^{''}$, $R_2^{''}$, and $R_5^{''}$ can be expressed as follows:

$$R_1^{''} = 0, \tag{20a}$$

$$R_2^{''} = -p_0^2 p_f^1 C(T - t_1) p_f^{2''} + 2p_0^2 p_f^1 C p_f^{2'} + p_0^2 p_f^1 C t_2 p_f^{2''}, \tag{20b}$$

$$R_5^{''} = -p_1 p_0 C\left(1 - p_f^1\right)(T - t_1) p_f^{2''} + 2p_1 p_0 C\left(1 - p_f^1\right) p_f^{2'} + p_1 p_0 C\left(1 - p_f^1\right) t_2 p_f^{2''}, \tag{20c}$$

where $p_f^{2'}$ and $p_f^{2''}$ are the first and second derivatives of $p_f^2$ in terms of $t_2$, respectively. According to Eq. (11), it can be obtained that $p_f^{2'} < 0$ and $p_f^{2''} > 0$. In addition, because $T - t_1 \geq t_2$, $R_2^{''} < 0$ and $R_5^{''} < 0$. Therefore, the relation $R_{total}^{''} = R_1^{''} + R_2^{''} + R_5^{''} < 0$ can be obtained, and thus $R_{total}$ is a concave function.

Then, the second derivative of $E_{total}$ can be calculated in the same manner as given below:

$$E_{total}^{''} = E_1^{''} + E_2^{''} + E_3^{''} + E_4^{''} + E_5^{''} + E_6^{''} + E_7^{''} + E_8^{''} + E_9^{''} + E_{10}^{''} + E_{11}^{''} + E_{12}^{''}, \tag{21}$$

where $E_{1-12}^{''}$ denote the second derivatives of $E_{1-12}$ in terms of $t_2$, respectively. According to the functions of $E_{1-12}$, $E_{1-12}^{''}$ can be expressed as follows:

$$E_1^{''} = 0, \tag{22a}$$

$$E_2^{''} = -p_0^2 p_f^1 (TE_t - t_1 E_t + t_1 E_s) p_f^{2''} - 2p_0^2 p_f^1 (E_s - E_t) p_f^{2'} - p_0^2 p_f^1 (E_s - E_t) t_2 p_f^{2''}, \tag{22b}$$

$$E_3^{''} = p_0^2 p_f^1 E_s t_1 p_f^{2''} + 2p_0^2 p_f^1 E_s p_f^{2'} + p_0^2 p_f^1 E_s t_2 p_f^{2''}, \tag{22c}$$

$$E_4^{''} = p_1 p_0 E_s t_1 \left(1 - p_f^1\right) p_f^{2''} + 2p_1 p_0 E_s \left(1 - p_f^1\right) p_f^{2'} + p_1 p_0 E_s \left(1 - p_f^1\right) t_2 p_f^{2''}, \tag{22d}$$

$$E_5^{''} = -p_1 p_0 \left(1 - p_f^1\right)(TE_t - t_1 E_t + t_1 E_s) p_f^{2''} - 2p_1 p_0 \left(1 - p_f^1\right)(E_s - E_t) p_f^{2'} - p_1 p_0 \left(1 - p_f^1\right)(E_s - E_t) t_2 p_f^{2''}, \tag{22e}$$

$$E_6^{''} = 0, \tag{22f}$$

$$E_7^{''} = 0, \tag{22g}$$

$$E_8^{''} = 0, \tag{22h}$$

$$E_9^{''} = 0, \tag{22i}$$

$$E_{10}^{''} = 0, \tag{22j}$$

$$E_{11}^{''} = 0, \tag{22k}$$

$$E_{12}^{''} = 0. \tag{22l}$$

Since $E_1^{''} = E_6^{''} = E_7^{''} = E_8^{''} = E_9^{''} = E_{10}^{''} = E_{11}^{''} = E_{12}^{''} = 0$, focusing on $E_2^{''}$, $E_3^{''}$, $E_4^{''}$, and $E_5^{''}$ leads to the following equations:

$$E_2^{''} + E_3^{''} = -p_0^2 p_f^1 E_t (T - t_1) p_f^{2''} + 2p_0^2 p_f^1 E_t p_f^{2'} + p_0^2 p_f^1 E_t t_2 p_f^{2''}, \tag{23}$$

$$E_4^{''} + E_5^{''} = -p_1 p_0 E_t \left(1 - p_f^1\right)(T - t_1) p_f^{2''} + 2p_1 p_0 E_t \left(1 - p_f^1\right) p_f^{2'} + p_1 p_0 E_t \left(1 - p_f^1\right) t_2 p_f^{2''}. \tag{24}$$

Since $E_2^{''} + E_3^{''} < 0$ and $E_4^{''} + E_5^{''} < 0$, $E_{total}^{''} < 0$ and as a result $E_{total}$ is also a concave function. In addition, $\frac{R_{total}^{''}}{E_{total}^{''}} = \frac{C}{E_t}$, where $\frac{C}{E_t}$ is a fixed positive number larger than 1 according to the predefined values in Table 2. This means $R_{total}$ and $E_{total}$ increase or decrease simultaneously, and the variation rate of $R_{total}$ is $\frac{C}{E_t}$ times of the variation rate of $E_{total}$.

**Table 2** Simulation parameters

| Parameters | Value |
|---|---|
| $p_d^{th}$ | 0.9 |
| $p_f^{th}$ | 0.1 |
| $T$ | 0.2 s |
| $W$ | 6 MHz |
| $\gamma$ | − 20 dB |
| $\gamma_s$ | 20 dB |
| $C$ | 6.6582 bits/sec/Hz |
| $E_s$ | 0.1 W |
| $E_t$ | 3 W |

Based on Eq. (17), the following equation can be obtained for $\eta(t)$:

$$\eta(t) = \frac{R_{total}(t)}{E_{total}(t)}, \tag{25}$$

$$\eta(t+\Delta t) = \frac{R_{total}(t+\Delta t)}{E_{total}(t+\Delta t)}, \tag{26}$$

where $\Delta t$ denotes the increased time. Therefore, the difference of $\eta(t+\Delta t)$ and $\eta(t)$ can be expressed as

$$\eta(t+\Delta t) - \eta(t) = \frac{R_{total}(t+\Delta t)}{E_{total}(t+\Delta t)} - \frac{R_{total}(t)}{E_{total}(t)}. \tag{27}$$

When both sides of Eq. (27) are multiplied by $\frac{E_{total}(t+\Delta t)}{R_{total}(t)}$, the following can be obtained.

$$\frac{E_{total}(t+\Delta t)}{R_{total}(t)}(\eta(t+\Delta t) - \eta(t)) = \frac{R_{total}(t+\Delta t)}{R_{total}(t)} - \frac{E_{total}(t+\Delta t)}{E_{total}(t)}. \tag{28}$$

As mentioned before, we have known that the variation rate of $R_{total}$ is $\frac{C}{E_t}$ times of the variation rate of $E_{total}$, and $\frac{E_{total}(t+\Delta t)}{R_{total}(t)}$ is positive. When $R_{total}$ and $E_{total}$ increase, $\frac{R_{total}(t+\Delta t)}{R_{total}(t)}$ becomes larger than $\frac{E_{total}(t+\Delta t)}{E_{total}(t)}$ and thus $\eta(t+\Delta t) - \eta(t) > 0$. When $R_{total}$ and $E_{total}$ decrease, $\frac{R_{total}(t+\Delta t)}{R_{total}(t)}$ becomes smaller than $\frac{E_{total}(t+\Delta t)}{E_{total}(t)}$ and thus $\eta(t+\Delta t) - \eta(t) < 0$. In other words, $\eta(t)$ increases when $R_{total}$ and $E_{total}$ increase and $\eta(t)$ decreases when $R_{total}$ and $E_{total}$ decrease. Therefore, $\eta(t)$ is also a concave function, and the optimal value of $t_2$ that maximizes the energy efficiency must exist.

In addition, MATLAB was also utilized to show that $\eta(t)$ is a concave function.

*Criteria* A function $f(x) : U \subset R \rightarrow R$ is concave if and only if its second derivative $f''(x) \leq 0$.

*Proof* The second derivative of $\eta(t)$ is calculated using MATLAB with $p_0 = 0.7$ and the parameters presented in Table 2. The result is presented in Fig. 4, which shows that the second derivative of $\eta(t_2)$ is always less than 0, and as a consequence, $\eta(t_2)$ is a concave function. Moreover, Fig. 4 shows that the range of $t_2$ is between 0.01 and 0.18.

The Golden Section Search method can be applied if a function $f(x)$ is continuous and unimodal within the interval $[a, b]$. The golden ratio can be used to determine location of two interior points within the interval $[a, b]$, and one of the interior points can be re-used in the next iteration. Thus, the approximation of extremum can be achieved by successively narrowing the interval in which the extremum lies on. In general, the Golden Section Search method is used to find the minimum. Thus, $-\eta(t_2)$ is minimized (which means the energy efficiency of the SU is maximized) to find the optimal value of $t_2$.

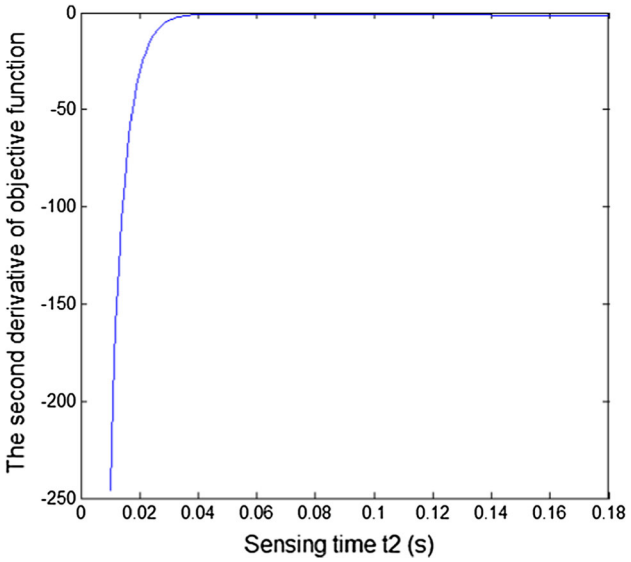


**Fig. 4** The second derivative of objective function $\eta$ as a function of sensing time $t_2$

The pseudo-code for the Golden Section Search method used in this paper is presented in Algorithm 1. In line 1, the lower and upper bounds of interval $a$ and $b$ and the error limit $\varepsilon$ are provided as input. Note that $\varepsilon$ should be a small value. $\lambda$ is the golden ratio ($\lambda = 1.6180\ldots$). Then, the interior points $a_1$ and $a_2$ within the interval $[a,b]$, and the corresponding values of $-\eta(a_1)$ and $-\eta(a_2)$ are calculated (line 3–4). In lines 5–9, a check is made to determine whether the new lower and upper bounds of the interval satisfy the condition $|a-b| \leq \varepsilon$. If the condition is satisfied, the optimal sensing time $t_2^*$ can be approximated as $1/2(a+b)$ (line 10); otherwise, the procedure repeats from line 5.

**Algorithm 1** The pseudo-code of the golden section search method

1: **procedure** GOLDEN_SEARCH_METHOD ($a$, $b$, $\varepsilon$)
2: $\lambda = 0.618$
3: $a_1 = b - \lambda(b-a)$, $y_1 = -\eta(a_1)$
4: $a_2 = a + \lambda(b-a)$, $y_2 = -\eta(a_2)$
5: **while** $|a-b| \geq \varepsilon$ **do**
6: **if** $y_1 > y_2$ **then**
7: $a = a_1$, $a_1 = a_2$, $a_2 = a + \lambda(b-a)$
8: **else**
9: $b = a_2$, $a_2 = a_1$, $a_1 = b - \lambda(b-a)$
10: **return** $t_2^* = \frac{1}{2}(a+b)$

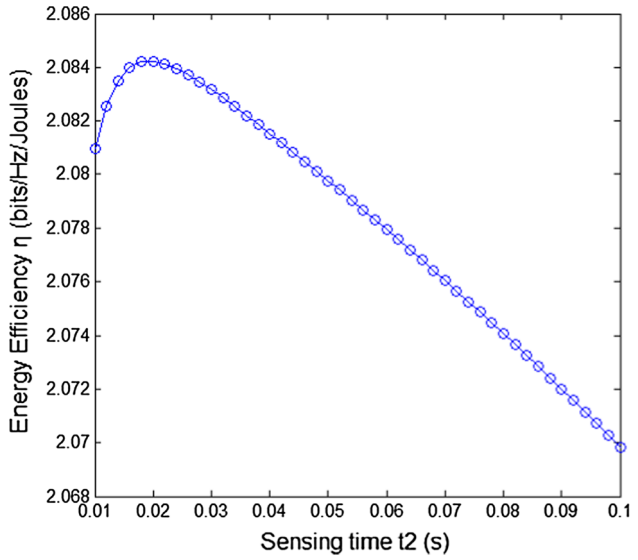


**Fig. 5** Energy efficiency $\eta$ as a function of sensing time $t_2$ with $p_0 = 0.7$

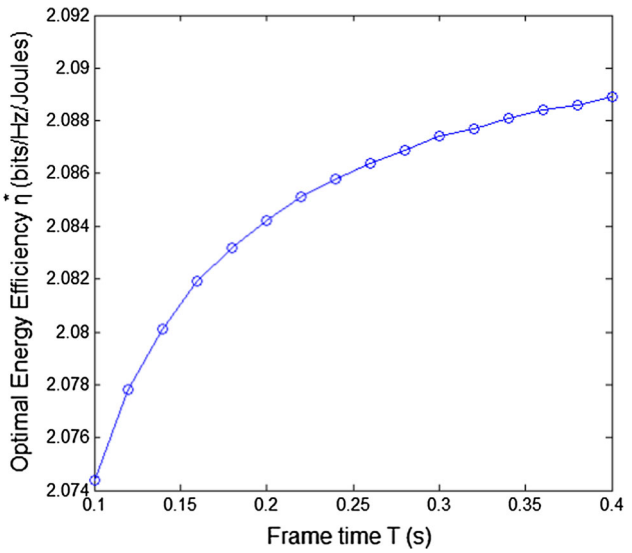


**Fig. 6** The optimal energy efficiency $\eta^*$ as a function of frame time $T$ with $p_0 = 0.7$

## 5 Performance evaluation

This section presents the performance evaluation of the proposed scheme using MATLAB. The performance of the proposed scheme is also compared with two other schemes proposed in [14, 19]. In addition, our simulation study considers varying levels of PU activity, which is in contrast to most prior work that simply perform simulations using a fixed level of PU activity.

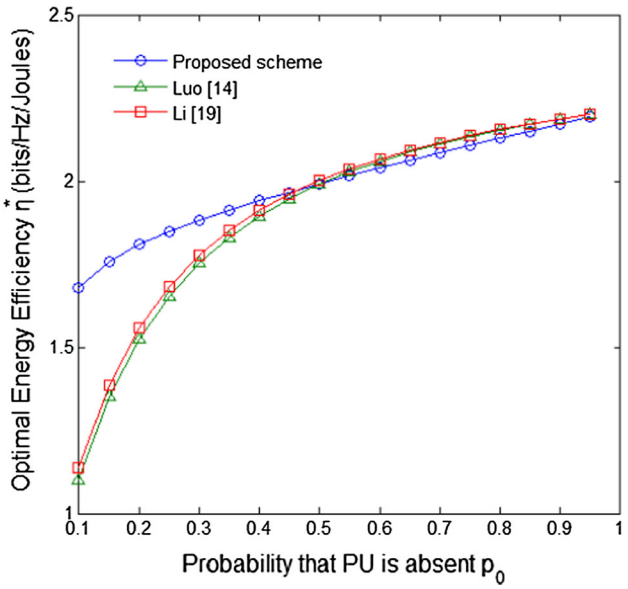


**Fig. 7** Comparison of the optimal energy efficiency as a function of $p_0$ and $T = 0.2$ s

### 5.1 Simulation parameters

The simulation environment is a CRSN with one PU and ten SUs that are allocated randomly within the communication range of the PU. The licensed band occupied by the PU is subdivided into ten non-overlapping sub-bands, which are assigned to the ten SUs. The parameters used in our simulations are shown in Table 2. The values of $p_d^{th}$ and $p_f^{th}$ are set according to the IEEE 802.22 cognitive radio wireless regional area network (WRAN) standard [28]. The frame length $T$ and the bandwidth of a sub-band $W$ are set as 0.2 s and 6 MHz, respectively. Since $\gamma_s$ is 20 dB, each SU has a channel capacity ($C$) of $\log_2(1+\gamma_s) =$ 6.6582 bits/sec/Hz. The level of PU activity is defined as the probability that PU is absent $p_0$, where $0 < p_0 < 1$. Finally, the energy consumed by spectrum sensing ($E_s$) and data transmission ($E_t$) for unit time are set to the same values as in [19].

### 5.2 Simulation results

Figure 5 shows the energy efficiency $\eta$ of the proposed scheme as a function of sensing time $t_2$ when $p_0 = 0.7$. Note that $p_0$ is fixed at 0.7 to show the variation of the energy efficiency as a function of $t_2$. The simulation results with varying $p_0$ will be shown in Figs. 7, 8 and 9. In Eq. (12), since $p_d^{th} = 0.9$, $p_f^{th} = 0.1$, $W = 6$ MHz, and $\gamma$ = -20 dB, the sensing period $t_1$ is the only unknown variable and can be calculated as 0.011 s. As can be seen, the energy efficiency at first increases as $t_2$ increases, and then after the optimal point, it decreases again. The main

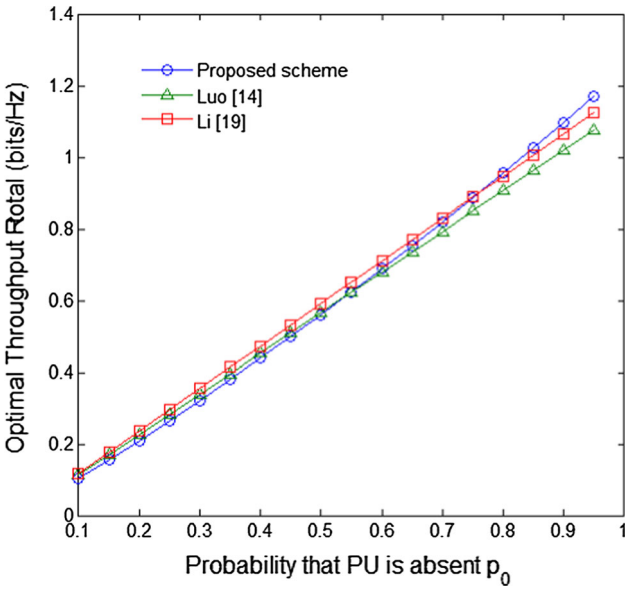


**Fig. 8** Comparison of the optimal secondary throughput as a function of $p_0$ and $T = 0.2$ s

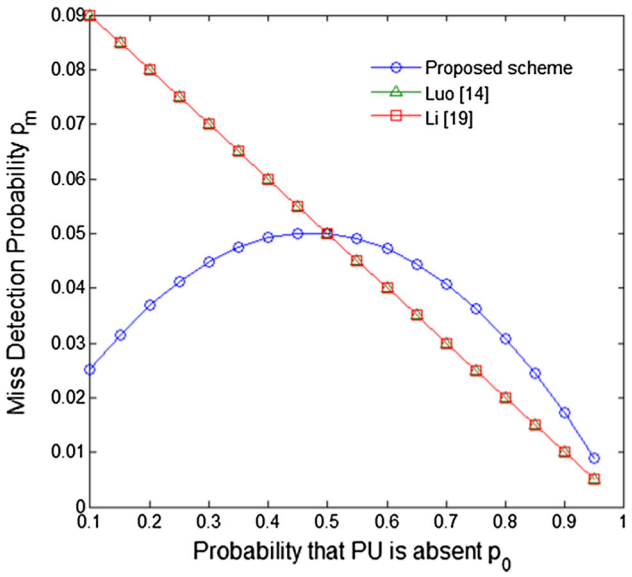


**Fig. 9** Comparison of the miss detection probability as a function of $p_0$ and $T = 0.2$ s

reason for this is that $p_d^2$ is also fixed at $p_d^{th}$, and therefore $p_f^2$ decreases as $t_2$ increases according to Eq. (11). During $t_2$, the probabilities of correcting false alarm and miss detection that occurred during $t_1$ are $1 - p_f^2$ and $p_d^{th}$, respectively, which improve energy efficiency. However, the time remaining for data transmission decreases as $t_2$ increases, which degrades network throughput. Therefore, after the optimal point for $t_2$, the energy efficiency decreases again, even though the sensing performance of $t_2$ improves. Figure 5 confirms that the objective function $\eta(t_2)$ is a concave function, and its optimal value that maximizes the network energy efficiency actually exists. Note that the false alarm probability $p_f^2$ is greater than $p_f^{th}$ when the sensing period is very short. In the next set of simulations, the optimal sensing period for $t_2$ will be obtained subjected to the requirement $p_f^2 \leq p_f^{th}$. Actually, because $t_2 \geq t_1$, the constraint $p_f^2 \leq p_f^{th}$ must be satisfied.

Figure 6 shows the optimal energy efficiency $\eta^*$ of the proposed scheme as a function of frame time $T$ when $p_0$ is fixed as 0.7. As can be seen, the optimal network energy efficiency of the proposed scheme increases with $T$. The reason is that in general miss detection and false alarm have a greater negative impact on energy efficiency when $T$ is longer. For example, if a miss detection occurs, the PU will be interfered by SUs' communications for a longer time as $T$ increases. If a false alarm occurs, the opportunities for SUs to achieve secondary throughput decreases as $T$ increases. However, these sensing errors can be corrected to some extent by the proposed scheme. Hence, energy efficiency can be improved when $T$ becomes longer.

Figure 7 compares the optimal energy efficiency $\eta^*$ of the proposed scheme against the methods proposed in [14, 19] as a function of $p_0$ (where $p_0$ is in the interval [0.1, 0.95]) with the frame length $T$ fixed at 0.2 s. As can be seen, the proposed scheme is much better than the other two schemes when PUs are more active. More specifically, when $p_0 = 0.1$, the energy efficiency of the proposed scheme is 52 and 47% higher than the methods proposed in [14, 19], respectively. As $p_0$ increases, the energy efficiency of the proposed scheme becomes slightly lower than the ones proposed in [14, 19]. When $p_0 = 0.7$, the energy efficiency of the proposed scheme is only 1.3 and 1.5% lower than the ones proposed in [14, 19], respectively. Furthermore, the energy efficiency of the proposed scheme is almost the same with the ones in [14, 19] when the value of $p_0$ becomes 0.95. These results clearly show that our proposed scheme is better when the varying PU activity is considered. The reason for this can be explained by Figs. 8 and 9.

Figure 8 shows that the secondary throughput results of these three schemes as a function of $p_0$ for $T$ fixed at 0.2 s. In the proposed scheme, even though the SUs may spend more time performing the second spectrum sensing, the network throughput can be improved when false alarms can be corrected. This is the reason why the throughput results of these three schemes are almost the same.

Figure 9 compares the miss detection probability $p_m$ of the three schemes as a function of $p_0$ for $T$ fixed at 0.2 s. Note that the methods proposed in [14, 19] have the same miss detection probability, denoted as $p_m^2$, as given below:

$$p_m^2 = p_1(1 - p_d), \quad (29)$$

Figure 9 shows that the miss detection probability of the proposed scheme is much lower than the ones proposed in [14, 19] when $p_0 < 0.5$. In particular, when $p_0 = 0.1$, the miss detection probabilities of the methods in [14, 19] are 257% higher than our proposed scheme. However, when $p_0 \geq 0.5$, the miss detection probability of the proposed scheme is slightly higher. When $p_0 = 0.7$, the miss detection probability of the proposed scheme is 36% higher than the other two schemes. Among the 12 cases, the cases 8, 10, and 11 can lead to miss detection. Therefore, the mathematical model for miss detection probability of the proposed method $p_m^1$ can be formulated as follows:

$$p_m^1 = p_1^2(1 - p_d)^2 + p_0 p_1(1 - p_d) + p_0 p_1 p_d(1 - p_d), \quad (30)$$

where the first, second, and third terms represent the probabilities of the cases 8, 10, and 11, respectively. Therefore, the difference between $p_m^1$ and $p_m^2$ can be calculated as

$$p_m^1 - p_m^2 = p_1 p_d(1 - p_d)(p_0 - p_1). \quad (31)$$

Since Fig. 8 shows that all of these three schemes have similar secondary throughputs, the energy consumption is the only factor that influence the energy efficiency. When $p_0 > 0.5$, the miss detection probability of the proposed scheme is a slightly higher than the ones in [14, 19], thus the energy consumed by invalid data transmission will be higher. When $p_0 < 0.5$, the miss detection probability of the proposed scheme is much lower than the ones in [14, 19]. Therefore, even though the proposed scheme spends more time to perform the second spectrum sensing when the first sensing result shows that the state of the PU has changed, there is a certain probability to that the miss detection can be corrected and thus provide better protection. This reduces the amount of invalid data transmissions performed by SUs, and decreases unnecessary energy consumption. This improves the network energy efficiency and prolongs the network lifetime.

## 6 Conclusion and future work

This paper proposed a novel spectrum sensing scheme for CRSNs. Based on the sensing result of the current frame, SU can dynamically decide to perform spectrum sensing for another period. The second spectrum sensing is performed to ensure the accuracy of the current sensing result if it is different from the previous sensing result. The first spectrum sensing period for the current frame can be calculated based on the detection probability and false alarm probability that satisfy the essential requirements of CRSNs. The second spectrum sensing period is optimized by optimizing network energy efficiency. In order to find the optimal second spectrum period, the Golden Section Search method is employed. Finally, our simulation study showed that the proposed scheme is more energy efficient than existing methods. As a future work, we plan to further improve the network energy efficiency by optimizing the frame length, and also consider the multicast of multichannel multiradio system combined with the CR technology [29].

**Acknowledgements** This research was supported by Basic Science Research Program through National Research Foundation of Korea (NRF) funded by the Ministry of Education (NRF-2013R1A1A2059741).

## References

1. Federal Communications Commission. (2003). *FCC, ET Docket No 03-222 Notice of proposed rule making and order*. Technical Report.
2. Mitola, J., & Maguire, G. Q. (1999). Cognitive radio: Making software radios more personal. *IEEE Personal Communications, 6*(4), 13–18.
3. Saifan, R., Kamal, A. E., & Guan, Y. (2012). Spectrum decision for efficient routing in cognitive radio network. In *Mobile Adhoc and Sensor Systems* (pp. 371–379).
4. Almasaeid, H. M., Jawadwala, T. H., & Kamal, A. E. (2010). On-demand multicast routing in cognitive radio mesh networks. In *Global Telecommunications Conference*.
5. Askari, M., Kavian, Y. S., Kaabi, H., & Rashvand, H. F. (2012). A channel assignment algorithm for cognitive radio wireless sensor networks. In *Wireless Sensor Systems (WSS)* (pp. 1–4).
6. Puccinelli, D., & Haenggi, M. (2005). Wireless sensor networks: Applications and challenges of ubiquitous sensing. *IEEE Circuits and Systems Magazine, 5*(3), 19–31.
7. Ewaisha, A., Sultan, A., & ElBatt, T. (2011). Optimization of channel sensing time and order for cognitive radios. In *Wireless Communications and Networking Conference (WCNC)* (pp. 1414–1419).
8. He, H., Li, G. Y., & Li, S. (2013). Adaptive spectrum sensing for time-varying channels in cognitive radios. *IEEE Wireless Communications Letters, 2*(2), 1–4.
9. Shokri-Ghadikolaei, H., Abdi, Y., & Nasiri-Kenari, M. (2012). Learning-based spectrum sensing time optimization in cognitive radio systems. In *Telecommunications (IST)* (pp. 249–254).
10. Sun, D., Song, T., Wu, M., Hu, J., Guo, J., & Gu, B. (2013). Optimal sensing time of soft decision cooperative spectrum sensing in cognitive radio networks. In *Wireless Communication and Networking Conference (WCNC)*.
11. Liu, X., Zhong, W., Ye, L., & Li, Q. (2013). Joint optimal sensing time and number of cooperative users in OR-RULE cooperative spectrum sensing. In *Wireless Communications & Signal Processing (WCSP)*.
12. Yin, W., Ren, P., & Zhang, C. (2011). A joint sensing-time adaption and data transmission scheme in cognitive radio networks. In *Global Telecommunications Conference (GLOBECOM)*.
13. Zhong, W., Chen, K., & Liu, X. (2017). Joint optimal energy-efficient cooperative spectrum sensing and transmission in cognitive radio. *China Communications, 14*(1), 98–110.

14. Luo, L., & Roy, S. (2012). Efficient spectrum sensing for cognitive radio networks via joint optimization of sensing threshold and duration. *IEEE Transactions on Communications, 60*(10), 2851–2860.
15. Deepak, G. C., & Navaie, K. (2013). On the sensing time and achievable throughput in sensor-enabled cognitive radio networks. In *Wireless Communication Systems (ISWCS)* (pp. 1–5).
16. Fu, J., Yibing, Z., Yi, L., Shuo, L., & Jun, P. (2015). The energy efficiency optimization based on dynamic spectrum sensing and nodes scheduling in cognitive radio sensor networks. In *Control and Decision Conference (CCDC)* (pp. 4371–4378).
17. Awin, F., Abdel-Raheem, E., & Ahmadi, M. (2017). Joint optimal transmission power and sensing time for energy efficient spectrum sensing in cognitive radio system. *IEEE Sensors Journal, 17*(2), 369–376.
18. Zhang, H., Nie, Y., Cheng, J., Leung, V. C. M., & Nallanathan, A. (2017). Sensing time optimization and power control for energy efficient cognitive small cell with imperfect hybrid spectrum sensing. *IEEE Transactions on Wireless Communications, 16*(2), 730–743.
19. Li, X., Cao, J., Ji, Q., & Hei, Y. (2013). Energy efficient techniques with sensing time optimization in cognitive radio networks. In *IEEE Wireless Communications and Networking Conference (WCNC)* (pp. 25–28).
20. Ghosh, C., Cordeiro, C., Agrawal, D. P., & Rao, M. B. (2009). Markov chain existence and hidden Markov models in spectrum sensing. In *Pervasive Computing and Communications*.
21. Farag, H. M., & Ehab, M. (2014). An efficient dynamic thresholds energy detection technique for cognitive radio spectrum sensing. In *Computer Engineering Conference (ICENCO)* (pp. 139–144).
22. Bai, X., Hao, M., & Wang, W. (2015). Frequency spectrum sensing of cognitive radio based on bayesian network. In *International Congress on Image and Signal Processing (CISP)* (pp. 1095–1099).
23. Lee, D.-J. (2015). Adaptive random access for cooperative spectrum sensing in cognitive radio networks. *IEEE Transactions on Wireless Communications, 14*(2), 831–840.
24. Urkowitz, H. (1967). Energy detection of unknown deterministic signals. *Proceedings of the IEEE, 55*(4), 523–531.
25. Proakis, J. G. (2006). *Digital communication* (4th ed.) (J Zhang etc., Trans.). Publishing House of Electronic Industry.
26. Lee, W.-Y., & Akyildiz, I. F. (2008). Optimal spectrum sensing framework for cognitive radio networks. *IEEE Transactions on Wireless Communications, 7*(10), 3845–3857.
27. Pei, Y., Liang, Y. C., Teh, K. C., & Li, K. H. (2011). Energy-efficient design of sequential channel sensing in cognitive radio networks: Optimal sensing strategy, power allocation, and sensing order. *IEEE Journal on Selected Areas in Communications, 29*(8), 1648–1659.
28. Stevenson, C. R., Chouinard, G., Lei, Z., Hu, W., Shellhammer, S. J., & Caldwell, W. (2009). IEEE 802.22: The first cognitive radio wireless regional area network standard. *Communications Magazine, IEEE* (Vol. 47, No. 1, pp. 130–138).
29. Fu, L., & Wang, X. (2013). Multicast scaling law in multichannel multiradio wireless networks. *IEEE Transactions on Parallel and Distributed Systems, 24*(12), 2418–2428.

**Fanhua Kong** received the B.E. degree in electronic and information engineering from Harbin Engineering University, China, in 2011, and he is currently pursuing the Ph.D. degree with the Department of Computer Engineering, Kyung Hee University, South Korea. His research interests include cognitive radio sensor networks.

**Zilong Jin** received the B.E. degree in computer engineering from Harbin University of Science and Technology, China, in 2009, and the M.S. and Ph.D. degrees in computer engineering from Kyung Hee University, Korea, in 2011 and 2016, respectively. He is currently an assistant professor of School of Computer and Software at Nanjing University of Information Science and Technology, China. His research interests include wireless sensor networks, mobile wireless networks, and cognitive radio networks.

**Jinsung Cho** received his B.S., M.S, and Ph.D. degrees in computer engineering from Seoul National University, Korea, in 1992, 1994, and 2000, respectively. He was a visiting researcher at IBM T.J. Watson Research Center in 1998 and a research staff at SAMSUNG Electronics in 1999–2003. Currently, he is a professor at Department of Computer Engineering, Kyung Hee University, Korea. His research interests include mobile system security, embedded security, IoT security, and sensor & body networks.

**Ben Lee** received the B.E. degree in electrical engineering from the Department of Electrical Engineering, State University of New York, Stony Brook, in 1984, and the Ph.D. degree in computer engineering from Department Electrical and Computer Engineering, Pennsylvania State University, in 1991. His research interests include multimedia streaming, wireless networks, embedded systems, computer architecture, multithreading and thread-level speculation, and parallel and distributed systems. He was a recipient of the Loyd Carter Award for Outstanding and Inspirational Teaching in 1994, the Alumni Professor Award for Outstanding Contribution to the College and the University from the OSU College of Engineering in 2005, and the HKN Innovation Teaching Award from Eta Kappa Nu, School of Electrical Engineering and Computer Science in 2008. He has been on the program committees and organizing committee for numerous international conferences including the 2005–2012 IEEE Workshop on Pervasive Wireless Networking, and the IEEE International Conference on Pervasive Computing and Communications (PerCom). He was the Workshop Chair for PerCom 2009. He was a Guest Editor for the Special Issue on Wireless Networks and Pervasive Computing of the Journal of Pervasive Computing and Communications. He was also an Invited Speaker at the 2007 International Conference on Embedded Software and System and a Keynote Speaker at the 2014 ACM International Conference on Ubiquitous Information Management and Communication. He is currently the TPC Chair at the 15th Annual IEEE Consumer Communications and Networking Conference (CCNC 2018). He is also an Adjunct Faculty Member from the Korea Advanced Institute of Science and Technology (KAIST).